AWARD NUMBER: W81XWH-20-1-0619

TITLE: Splice Ablation Kinase Inhibition (SAKI) of Receptor Tyrosine Kinases

PRINCIPAL INVESTIGATOR: Timothy Robinson, MD, PhD

CONTRACTING ORGANIZATION: H. Lee Moffitt Cancer Center & Research Institute

REPORT DATE: JULY 2022

TYPE OF REPORT: Final Report

PREPARED FOR: U.S. Army Medical Research and Development Command
Fort Detrick, Maryland 21702-5012

DISTRIBUTION STATEMENT: Approved for Public Release;
Distribution Unlimited

The views, opinions and/or findings contained in this report are those of the author(s) and should not be construed as an official Department of the Army position, policy or decision unless so designated by other documentation.

REPORT DOCUMENTATION PAGE

Form Approved
OMB No. 0704-0188

1. REPORT DATE	**2. REPORT TYPE**	**3. DATES COVERED**
JULY 2022	Final Report	8/15/2020 – 3/31/2022

4. TITLE AND SUBTITLE

Splice Ablation Kinase Inhibition (SAKI) of Receptor Tyrosine Kinases

5a. CONTRACT NUMBER
W81XWH-20-1-0619

5b. GRANT NUMBER
LCRP Award 190605

5c. PROGRAM ELEMENT NUMBER

6. AUTHOR(S)

Timothy Robinson, MD, PhD

E-Mail: timothy.j.robinson@yale.edu

5d. PROJECT NUMBER

5e. TASK NUMBER

5f. WORK UNIT NUMBER

7. PERFORMING ORGANIZATION NAME(S) AND ADDRESS(ES)

H. Lee Moffitt Cancer Center & Research Institute
Department of Radiation Oncology
MCC-RadOnc
12902 Magnolia Drive

8. PERFORMING ORGANIZATION REPORT

9. SPONSORING / MONITORING AGENCY NAME(S) AND ADDRESS(ES)

U.S. Army Medical Research and Development Command
Fort Detrick, Maryland 21702-5012

10. SPONSOR/MONITOR'S ACRONYM(S)

11. SPONSOR/MONITOR'S REPORT NUMBER(S)

12. DISTRIBUTION / AVAILABILITY STATEMENT

Approved for Public Release; Distribution Unlimited

13. SUPPLEMENTARY NOTES

A note regarding the delay of this report. The PI (Robinson) left Moffitt (last day 3/31/2022) after being recruited to Yale University (4/1/2022), at which point the remaining career development award funds were relinquished to the DOD. The DOD had sent notifications regarding the need for the final report to the PI's Moffitt email after 3/31/2022. However, Moffitt had removed PI access to Moffitt email and these notifications were not received regarding the final report, leading to the delay of this final report. Emails were recently forwarded to the PI's new institution and the reported completed within 30 days.

14. ABSTRACT

This final report describes the progress made towards the use of antisense oligonucleotides (ASOs) as a tool to drive splicing-based inhibition of the Epidermal Growth Factor Receptor (EGFR). Through this project we have confirmed the ability of EGFR-directed ASOs to inhibit EGFR signaling, decrease proliferation and survival, and drive a program of proteomic expression that mirrors that caused by erlotinib. Furthermore, we showed that the ASO-based approach works in both tyrosine kinase resistant and sensitive cell models, and to a less extent in wild type, EGFR-overexpressing lung cancer cell line models. This work was published in the journal of Nucleic Acid Therapeutics (Impact factor 4.2).

15. SUBJECT TERMS

NONE LISTED

16. SECURITY CLASSIFICATION OF:			**17. LIMITATION OF ABSTRACT**	**18. NUMBER**	**19a. NAME OF RESPONSIBLE PERSON** USAMRDC
a. REPORT	**b. ABSTRACT**	**c. THIS PAGE**			**19b. TELEPHONE NUMBER** *(include area code)*
U	U	U	UU	28	

Standard Form 298 (Rev. 8-98)
Prescribed by ANSI Std. Z39.18

TABLE OF CONTENTS

1. Introduction

The development of targeted small molecule drugs has revolutionized the treatment of many cancers by selectively targeting key driver oncogenes. However, the durability of molecularly targeted agents is limited by the development of resistance, often via protein-altering secondary mutations. In this project, we proposed a novel therapeutic paradigm that side-steps protein mutation-driven resistance by targeting oncogenes at the mRNA level using an approach we call "**Splice-Ablation Kinase Inhibition**", or "**SAKI**". SAKI manipulates alternative mRNA splicing by targeting specific pre-mRNA sequences to splice out exons located in key oncogene domains to: A) attack oncogenes at the mRNA level, (B) directly inhibit expression of functional oncogenes, and C) replace it with dominant negative variants that act to further antagonize oncogene signaling. Splicing-targeted therapy represents an entirely new category of antineoplastic agents and is a paradigm shift from current small molecules and antibodies, which target oncogenes at the protein level. A splicing-based antineoplastic therapy has many potential advantages, including the ability to do the following: (i) bypass entire exons harboring driver and resistance mutation hotspots within activating kinase or other signaling domains, (ii) target oncogenes with currently undruggable protein structures, (iii) drive expression of dominant negative decoy proteins, which may further inhibit oncogene-binding partners, (iv) create soluble decoys for membrane-bound onocogenes that are capable of paracrine inhibition in bystander or stromal cells, and (v) preferentially inhibit pathologically over-expressed (OE) genes for which splicing regulation is less robust. Although potentially applicable to virtually any oncogene, in this project we use SAKI to target the Epidermal Growth Factor Receptor (EGFR) in non-small cell lung cancer (NSCLC).

2. Keywords

Receptor Tyrosine Kinase, Tyrosine Kinase Inhibitors, Antisense Oligonucleotides, Epidermal Growth Factor Receptor, Exon skipping

3. Accomplishments

- ***What were the major goals of the project? What was accomplished under these goals?***

The accomplishments of the project are provided within the attached publication, which provides detailed technical descriptions and the experimental results. Below the specific accomplishments are summarized in narrative form.

Major Task 1: To develop the therapeutic potential of SAKI therapy in EGFR-driven NSCLC: We will test the hypothesis that EGFR-SAKI can be used to augment current treatment paradigms in NSCLC

Subtask 1 (0-12 months): To assess the potential therapeutic use of SAKI in *EGFRmt NSCLC*
We will explore several potential avenues by which SSOs may be used to augment current therapeutic treatments in EGFRmt NSCLC.

i) Direct SSO +/- TKI synergy: We will investigate SSO monotherapy as well as in combination with TKIs. We will use EGFRmt, addicted NSCLC adenocarcinoma cells to investigate the ability of SSOs to augment inhibition of EGFR signaling and resultant phenotypes.
Cell lines to be used: human PC9 and PC9GR cells, human HCC4006 and HCC4006ER cells

ACCOMPLISHED (100% COMPLETE): We confirmed the ability of direct SSOs to provide an in vitro therapeutic effect in EGFRmt NSCLC as assessed through cell viability and wound scratch assays in PC9 and PC9-GR cell lines. We found that EGFR ASOs were not effective in HCC4006 models, for unclear reasons.

ii) SSO targeting of Microenvironment: We will conduct co-culture experiments of TKI resistance, which have been conducted successfully at our institution by collaborators and demonstrate the role of tumor associated fibroblasts in TKI resistance. Cell lines to be used: human PC9 and IMR-90 cells

ACCOMPLISHED (80% COMPLETE): We have exposed different cell lines representative of the tumor microenvironment and normal stroma to EGFR-ASOs in vitro with mixed results. ASOs were able to drive exclusion of exons within IMR-90 cells. Although in vitro experiments demonstrated changes in the splicing of normal tissue representative cell types, minimal impacts on growth rate and survival were observed. Although there were initially plans to co-culture IMR-90 and PC-9 cells, we ultimately discontinued this line of research due to the early termination of the project.

Subtask 2 (3-12 months): To assess the potential therapeutic use of SAKI in WT-OE EGFR NSCLC.
We will characterize the potential therapeutic benefit of EGFR-SSOs for use in Wild-type, over-expressed NSCLC. Cell lines to be used: human H292 and H322 cells

ACCOMPLISHED (100% COMPLETE): We have confirmed the ability of direct SSOs to provide an in vitro therapeutic effect in H292 NSCLC as assessed through cell viability and wound scratch assays (figures 3a and supplemental figure 5a in attached manuscript draft). We found that EGFR ASOs were not effective in driving exon exclusion or phenotypic inhibition in H322 models, for unclear reasons.

Subtask 3 (12-24 months): To assess preliminary in vivo toxicity and efficacy. Observe the long-term toxicity and efficacy of SSO therapy at the systemic level. Mouse model: PC9 nude mice xenografts

ACCOMPLISHED (25% COMPLETE): We completed mouse model training and had begun drafting our protocol to use nude mice (NOD SCID) for xenograft experiments with PC9 and PC9-GR. In discussions with other collaborators, we discussed many details of these experiments with respect to the timing, dosing, and evaluation. However, mouse models were not conducted due to the early termination of the project associated with switching institutions.

Major Task 2: To Characterize the Specificity, Mechanism, and Regulation of EGFR-SAKI:

We will test the hypothesis that EGFR-SAKI splicing is highly specific, results in protein expression of dominant negative EGFR, and acts in part by blocking trans-acting splice factors.

Subtask 1 (6-18 months): To asses SAKI specificity.

i) Specificity (exon-specific knockdown): Specificity will be confirmed via EGFR exogenous rescue using a cDNA EGFR expression construct that lacks exons and therefore will be immune to splicing-based interventions. Cell lines to be used: human H292 cells

ACCOMPLISHED (50% COMPLETE): We worked extensively to construct cDNA EGFR constructs that lack exon 18. Unfortunately, cloning and selecting for stable expression of the EGFRex18 cDNA provided technically challenging for unclear reasons. We attempted this for several months but were ultimately unable to create stable lines expressing the exon 18 lacking EGFR isoform.

ii) RNA-seq: Cell lines to be used: human H292 cells

ACCOMPLISHED (100% COMPLETE): In order to conduct genome-wide characterization of ASO-induced changes, we elected to use mass spectroscopy proteomic analysis to compare the impact of SAKI vs. erlotinib on PC9 cell signaling. This was chosen in order to focus what was likely the most important endpoint of EGFR signaling (i.e. protein expression vs. mRNA expression). We treated ASOs targeting exons 16, 18, and 21 vs. ASO controls and identified subsequent proteomic and phosphoproteomic changes. Pathways enriched by EGFR-targeted ASOs were then compared to the effects of erlotinib compared with ASO controls. Phosphoproteomic mass spectrometry in PC9 cells pathway enrichment of differentially expressed proteins significantly (p-value < $10e^{-10}$) indicated ASO- and erlotinib-induced changes in cell cycle, mitosis, and G2/M checkpoint inhibition pathways. Proteomic analysis revealed that 13 out of 14 upregulated pathways and 4 out of 8 down regulated pathways overlapped in ASO-treated and erlotinib-treated PC9 cells, including cell growth related pathways such as DNA replication, transcription, and the cell cycle. Interestingly, phosphoproteomic pathway enrichment showed that several pathways related to cell growth were significantly downregulated in both ASO treated and Erlotinib treated PC9 cells, whereas most of these down regulated pathways were up regulated according protein expression. In addition to these pathways, proteins involved in apoptosis and apoptotic cleavage pathways were hyper-phosphorylated, further confirming the involvement of cell growth. The EGFR downstream signaling pathway was significantly hypo-phosphorylated in cells treated with EGFR ASOs, confirming EGFR-specific inhibition by EGFR-targeted ASO treatment. Most phosphorylation sites on EGFR were hypo-phosphorylated following both ASO and erlotinib treatment

iii) In vitro toxicity/survival of non-cancerous cell lines: Cell lines to be used: human HUVECs and Beas2B cells

ACCOMPLISHED (100% COMPLETE): Both HUVECs and Beas2B cells have been exposed to ASOs targeting exons 16, 18, and 21. ASOs did not result in splice-switching or a reduction in cell viability in HUVECs or Beas2B cells.

iv) Growth inhibition of non-EGFR dependent NSCLC: Cell lines to be used: human H358 and H441cells

ACCOMPLISHED (100% COMPLETE): Human H358 and H441 cells were exposed to ASOs in vitro and measured the cell viability. However, we detected significant off-target effects of our negative scramble control. The company-provided control showed no off-target effects. The ASOs had limited impact on growth of both cell lines, consistent with an EGFR-specific mechanism of inhibition.

Subtask 2 (6-18 months): To confirm EGFR dominant negative protein expression. Expression will be confirmed via (i) mass spectroscopy and gel-shift assays, (ii) followed by assessment of hetero-dimerization with other EGFR-family oncogenes (HER2-4) via co-immunoprecipitation and proximity ligation assays (PLA). Cell lines to be used: human PC9 and PC9GR cells, human H292 cells

ACCOMPLISHED (50% COMPLETE): We have conducted mass spectroscopy and gel-shift assays with the goal of confirming the expression of an EGFR isoform that lacks the targeted exons (16, 18, and 21). However, we have not been able to detect peptides that are unique to the predicted isoforms. This has been technically challenging due to the small change in protein content that results from only a single exon being excluded and results in relatively few unique peptides that can be detected by mass spectroscopy. Attempting to confirm changes in length by gel-shift assay was also technically complicated by antibodies with proprietary target domains and the presence of non-specific bands by Western blot.

Recent publications have shed some light on the challenges we experienced, most notably by Adrian Krainer's lab at Cold Spring Harbor, which was learned about in part through the Cold Spring Harbor experience provided by the DOD career development grant. It appears that ASO-based manipulation of mRNA splicing can trigger nonsense-mediated decay of the targeted gene. Therefore, although our ASOs targeted against EGFR were able to drive exon exclusion at the mRNA level, we were never able to confirm protein-level expression of the exon 18 lacking variant. This may be due to nonsense-mediated decay. However, it is possible that there may be still future therapeutic potential, since additional ASOs may be designed to block exon-junction complexes and therefore inhibit gene-specific nonsense-mediated decay. This would be an excellent topic of potential future research regarding any ASO-based anti-neoplastic approach.

Reference: Gene-specific nonsense-mediated mRNA decay targeting for cystic fibrosis therapy
Young Jin Kim, Tomoki Nomakuchi, Foteini Papaleonidopoulou, Lucia Yang, Qian Zhang & Adrian R. Krainer
Nature Communications volume 13, Article number: 2978 (2022)

Subtask 3 (12-24 months): To identify trans-acting splicing factors. Factors will be identified via mass spec of WT EGFR pre-mRNA pull down of targeted exons (16 &18) pre- and post- SAKI. We will investigate the presence of RNA-binding proteins within the targeted pre-mRNA EGFR exons. Cell lines to be used: human H292 and H322 cells

ACCOMPLISHED (0% COMPLETE): Ultimately this task was abandoned following the inability to confirm protein-level expression of EGFR splicing variants that lacked the exons 16 or 18.

- ***What opportunities for training and professional development has the project provided?***

Abstract submission and participation at the 2021Cold Spring Harbor Labs (CSHL) eukaryotic mRNA processing workshop. This opportunity was critical to introducing me to the concept of nonsense-mediated decay of ASO-targeted therapeutics and also highlighted challenges in using murine models and solid tumor models of ASO-based therapies, which remained complicated by challenges in drug delivery.

Expertise with ASOs to manipulate target gene splicing

Professional development through novel collaborations using splicing to enhance NSCLC immune therapy, which may largely avoid challenges with ASO drug delivery to solid tumors.

Regular discussions with mentors has provided increased knowledge of proteomics and phosphoproteomics analysis, including the use of mass spectroscopy to attempt to identify alternatively splice protein isoforms.

I was ultimately recruited to Yale University, which has one of the world's largest RNA-centers. I have a small damp translational lab that is continuing my work in alternative splicing in cancer, largely thanks to the support provided by the DOD career development grant.

- ***How were the results disseminated to communities of interest?***

A manuscript has been published in the journal Nucleic Acid Therapeutics (Impact factor 4.244), which summarizes nicely all the key findings observed as part of this supported research.

- ***What do you plan to do during the next reporting period to accomplish the goals?***

This is the final report. No further work is currently planned in EGFR, however, the lessons learned and techniques developed are being applied to therapeutic splicing related to immune therapy and in hematologic malignancies, both of which are ongoing topics of research.

4. Impact

- ***What was the impact on the development of the principal discipline(s) of the project?***

The ability to design custom ASOs to drive exclusion of target exons provides an opportunity to target additional oncogenes or immune checkpoints in the future. The confirmation that the ASOs can be used to inhibit EGFR signaling, independent of EGFR TKIs, provides evidence that this approach to target oncogenes using splicing modifications may have a future therapeutic potential.

- ***What was the impact on other disciplines?***

The ability to target any gene with splicing may offer a novel opportunity to target genes involved in immune checkpoint regulation, which could include internal/intracellular factors that cannot be targeted using current antibody approaches.

- ***What was the impact on technology transfer?***

Nothing to report

- ***What was the impact on society beyond science and technology?***

Nothing to report

5. Changes/Problems

- ***Changes in approach and reasons for change***

A fundamental challenge of ASO-based therapy, found through our experiments and in discussions with others in the field, is that ASO-based therapy can trigger nonsense-mediate decay of the target gene. Although this was still able to drive EGFR-based inhibition, we were never able to confirm expression of a dominant negative EGFR gene at the protein level that lacked exons 16 or 18. We attempted this through mass-spec, focusing on predicted neo-peptides that would be unique to the novel isoforms, but were not able to detect these peptides. We also attempted to detect size-shift by Western blot, but this was also not successful as no second band was observed. As mentioned above, there are evolving methods using ASOs that may be able to counteract nonsense-mediated decay currently being studied. In addition, discussions with others in the field raised concerns about the ability of ASOs to penetrate solid tumors (i.e., lung cancers). Although we never confirmed a lack of response, this stifled concerns about pursuing the use of ASOs for solid tumors as a focal point of my future long-term career. I have since shifted focus to immune therapy and hematologic malignancies, where drug penetration of solid tumors is thought to be less of a concern.

- ***Actual or anticipated problems or delays and actions or plans to resolve them***

We have had difficulty proving the expression of the aberrantly spliced EGFR isoforms. Specifically, we have conducted mass spectroscopy and gel-shift assays with the goal of confirming the expression of an EGFR isoform that lacks the targeted exons (16, 18, and 21). However, we have not been able to detect peptides that are unique to the predicted isoforms. This has been technically challenging due to the small change in protein content that results from only a single exon being excluded and results in relatively few unique peptides that can be detected by mass spectroscopy. Attempt to confirm changes in length by gel-shift assay have also been technically complicated by antibodies with proprietary target domains and the presence of non-specific bands by Western blot.

- ***Changes that had a significant impact on expenditures***

Nothing to report

- ***Significant changes in use or care of human subjects, vertebrate animals, biohazards, and/or select agents***

Murine models were not performed prior to the early termination of the project due to the PI changing institutions.

- ***Significant changes in use or care of human subjects***

Nothing to report

- ***Significant changes in use or care of vertebrate animals.***

Nothing to report

- ***Significant changes in use of biohazards and/or select agents***

Nothing to report

6. Products

- ***Publications, conference papers, and presentations***

Final report bibliography:

Abstracts and conference presentations:

Madanayake TW, Haura EB, **Robinson TJ**. A novel approach to inhibit Epidermal Growth Factor Receptor (EGFR) signaling through Splice Switching Oligonucleotides (SSOs). Cold Spring Harbor Labs: Eukaryotic mRNA processing. August 2021. Abstract

Peer-reviewed manuscripts:

Inhibition of Epidermal Growth Factor Receptor Signaling by Antisense Oligonucleotides as a Novel Approach to Epidermal Growth Factor Receptor Inhibition. Thushara W. Madanayake, Eric A. Welsh, Lancia N.F. Darville, John M. Koomen, Charles E. Chalfant, Eric B. Haura, and **Timothy J. Robinson**. Nucleic Acid Therapeutics Vol. 32, No. 5. PMID: 35861718 PMCID: PMC9595651 DOI: 10.1089/nat.2021.0101

- ***Other products***

Research material created includes:

Custom ASO morpholinos targeting EGFR exons 16, 18, and 21
Custom RT-PCR primers to detect the above splicing events
cDNA of an expression construct with EGFR lacking exon 18

7. Participants & Other Collaborating Organizations

- ***What individuals have worked on the project? This final report notes the two individuals below who were supported by this research:***

Name:	*Thushara Madanayake*
Project Role:	*Post-doctoral researcher*
Researcher Identifier (e.g. ORCID ID):	*N/A*

Nearest person month worked:	18
Contribution to Project:	*Dr. Madanayake has conducted or assisted with all the reported bench work contained in this report*
Funding Support:	N/A

Name:	*Timothy Robinson*
Project Role:	*Principle Investigator*
Researcher Identifier (e.g. ORCID ID):	*0000-0003-0021-0668*
Nearest person month worked:	18
Contribution to Project:	*Dr. Robinson directed the research and was responsible for the conduct and design of experiments and resulting publication*
Funding Support:	N/A

- ***Has there been a change in the active other support of the PD/PI(s) or senior/key personnel since the last reporting period?***

Nothing to report

- ***What other organizations were involved as partners?***

Nothing to report

8. Special Reporting Requirements

Nothing to report

9. Appendix – Published Manuscript – Nucleic Acid Therapeutics

NUCLEIC ACID THERAPEUTICS
Volume 32, Number 5, 2022

DOI: 10.1089/nat.2021.0101

Inhibition of Epidermal Growth Factor Receptor Signaling by Antisense Oligonucleotides as a Novel Approach to Epidermal Growth Factor Receptor Inhibition

Thushara W. Madanayake,[1] Eric A. Welsh,[2] Lancia N.F. Darville,[3] John M. Koomen,[4] Charles E. Chalfant,[5,6] Eric B. Haura,[1] and Timothy J. Robinson[7]

We report a novel method to inhibit epidermal growth factor receptor (EGFR) signaling using custom morpholino antisense oligonucleotides (ASOs) to drive expression of dominant negative mRNA isoforms of EGFR by ASO-induced exon skipping within the transmembrane (16) or tyrosine kinase domains (18 and 21). *In vivo* ASO formulations induced >95% exon skipping in several models of nonsmall cell lung cancer (NSCLC) and were comparable in efficacy to erlotinib in reducing colony formation, cell viability, and migration in EGFR mutant NSCLC (PC9). However, unlike erlotinib, ASOs maintained their efficacy in both erlotinib-resistant subclones (PC9-GR) and wild-type overexpressing EGFR models (H292), in which erlotinib had no significant effect. The most dramatic ASO-induced phenotype resulted from targeting the EGFR kinase domain directly, which resulted in maximal inhibition of phosphorylation of EGFR, Akt, and Erk in both PC9 and PC9GR cells. Phosphoproteomic mass spectrometry confirmed highly congruent impacts of exon 16-, 18-, and 21-directed ASOs compared with erlotinib on PC9 genome-wide cell signaling. Furthermore, *EGFR*-directed ASOs had no impact in EGFR-independent NSCLC models, confirming an EGFR-specific therapeutic mechanism. Further exploration of synergy of ASOs with existing tyrosine kinase inhibitors may offer novel clinical models to improve EGFR-targeted therapies for both mutant and wild-type NSCLC patients.

Keywords: receptor tyrosine kinase, tyrosine kinase inhibitors, antisense oligonucleotides, epidermal growth factor receptor, exon skipping

Introduction

Receptor tyrosine kinases (RTKs) are cell surface proteins that belong to a subclass of tyrosine kinases [1]; they regulate a range of fundamental cellular processes pertinent to cancer progression, including cell proliferation, apoptosis, and migration [2]. RTKs contain an extracellular domain with ligand binding sites, a transmembrane domain, and an intracellular kinase domain [3]. Under normal physiological conditions, epidermal growth factor receptor (EGFR) is activated by ligand-induced dimerization and autophosphorylation of the intracellular kinase domain. In the cancer setting, EGFR signaling can become constitutively activated through kinase domain point mutations or deletions (lung cancer), deletion of the extracellular domain (malignant glioma), or amplification and overexpression (breast, head and neck, and lung cancer) [4]. Current EGFR therapies include the use of extracellularly targeted monoclonal antibodies (mAb; cetuximab, panitumumab) and intracellularly targeted tyrosine kinase inhibitors (TKIs; osimertinib, erlotinib, gefitinib, afatinib, neratinib, vandetanib, and lapatinib) [5,6].

First-generation TKIs (erlotinib and gefitinib) were the first agents to provide a therapeutic benefit in patients with nonsmall cell lung cancer (NSCLC) with *EGFR* mutations,

Departments of [1]Thoracic Oncology, [2]Biostatistics and Bioinformatics, [3]Proteomics and Metabolomics Core, [4]Molecular Oncology, H. Lee Moffitt Cancer Center and Research Institute, Tampa, Florida, USA.
[5]Department of Cell Biology and Medicine, School of Medicine, University of Virginia, Charlottesville, Virginia, USA.
[6]Research Service, James A. Haley Veterans' Administration Hospital, Tampa, Florida, USA.
[7]Department of Therapeutic Radiology, Yale School of Medicine, New Haven, Connecticut, USA.

providing a year of progression-free survival with a 30-month overall survival [7]. However, virtually, all patients eventually develop treatment resistance [7,8]. Second-generation EGFR TKIs (afatinib and dacomitinib) provided the first effective treatment of patients with resistance due to T790M mutations, made further effective by the third-generation TKI, osimertinib [9]. Again, these patients ultimately develop resistance (eg, C797S mutation) [10] and fourth-generation TKIs are being tested to provide efficacy in this setting, which will undoubtedly promote yet a further cycle of resistance and need for novel therapies.

Furthermore, TKIs only demonstrate a therapeutic benefit for the 10% to 20% of NSCLC patients whose tumor harbors an EGFR mutation. Far more NSCLC tumors, ~60%, exhibit overexpression of the wild-type *EGFR* gene (WT-OE) [11], for which no effective anti-EGFR therapy exists.

To address these existing shortcomings, we have investigated an alternative route of EGFR inhibition by the manipulation of alternative mRNA splicing, a critical and underappreciated phenomenon that contributes to cancer phenotypes [12]. We previously detected endogenously regulated EGFR-dominant negative isoforms [13], leading us to the hypothesis that EGFR inhibition can be regulated by alternative splicing. Antisense oligonucleotides (ASOs) have been previously designed to inhibit function by the manipulation of alternative splicing in *Bcl-x*, *HER2*, and *EGFR* mRNA [14–16], but have not been previously used to target *EGFR* pre mRNA. ASOs have now been clinically implemented as an effective and FDA-approved therapy used to treat spinal and Duchenne muscular dystrophy [17–19], demonstrating a potential therapeutic opportunity for ASO-based treatments.

In this study, we describe a novel approach to EGFR inhibition using custom phosphorodiamidate morpholino-based ASOs to (1) induce aberrant splicing of inhibitory isoforms of EGFR through a mechanism we refer to as splicing ablation kinase inhibition (SAKI), (2) demonstrate efficacy of SAKI-induced changes in oncogenic phenotype, EGFR signaling, and global phosphoproteomic expression analyses that mirror TKI treatment, and (3) demonstrate the efficacy of SAKI in both TKI-resistant EGFRmt NSCLC and EGFR WT-OE cell models.

Materials and Methods

Cells

For these studies, we used three NSCLC cell lines: human lung mucoepidermoid carcinoma cells (H292), the EGFRmt human lung adenocarcinoma cell line (PC-9), and the EGFRmt and gefitinib-resistant (T790M) human lung adenocarcinoma cell line (PC9-GR). These cells were provided by the Moffitt Lung Cancer Center of Excellence Cell Line Core.

Materials

ASOs/Morpholinos (Gene Tools, Philomath, OR); RPMI 1640 medium (Life Technologies Gibco, Grand Island, NY); fetal bovine serum (Life Technologies Gibco); trypsin-EDTA (0.05%) with phenol red (Life Technologies Gibco); Dulbecco's phosphate-buffered saline (PBS; Life Technologies Gibco); Platinum Hot-Start PCR Master Mix (Cat# 1300012; Invitrogen, Carlsbad, CA); high-capacity cDNA reverse transcription Kit (Cat# 4368813; Applied Biosystems, Foster City, CA); Macherey Nagel nucleospin RNA/Protein isolation kit (Cat# 740933; Bethlehem, PA); CellTiter-Glo luminescent cell viability assay (Cat# G7570; Promega, Madison, WI); 0.1% crystal violet; and Super-Signal West Pico plus chemiluminescent substrate (Thermo Fisher, Rockford, IL); Phospho-EGF Receptor (Tyr1068) (D7A5) XP Rabbit mAb (Cat# 2234; Cell Signaling, Danvers, MA); Phospho-Akt (Ser473) (D9E) XP Rabbit mAb (Cat# 9271; Cell Signaling); Phospho-p44/42 MAPK (Erk1/2) (Thr202/Tyr204) antibody (Cat# 9101; Cell Signaling); and EGF receptor (D38B1) XP Rabbit mAb (Cat# 4267; Cell Signaling).

Reverse transcriptase–polymerase chain reaction

Cells were seeded in six-well plates for ~24 h and treated with ASOs and controls. Treated cells were trypsinized and cell pellets were made. RNA was isolated using the Macherey Nagel nucleospin RNA/Protein isolation kit (Cat# 740933), according to the manufacturer's recommendations. RNA was quantified using the Nanodrop 1000 (Thermo Fisher), and 1,000 ng of RNA was used to make cDNA, which was synthesized using a high-capacity cDNA reverse transcription Kit (Cat# 4368813; Applied Biosystems) as per the manufacturer's instructions. Polymerase chain reaction (PCR) was performed with the Platinum hot start PCR master mix (Cat# 13000013; Invitrogen) using the respective primers. Resulted PCR products were run on agarose gel to visualize the bands.

Optimizing ASOs

Custom 25 bp morpholino ASOs were designed to drive the skipping of EGFR exons 16 (EGFRΔex16), 18 (EGFRΔex18), and 21 (EGFRΔex21), by targeting the 3′ and 5′ splice junction of each exon. ASO sequence optimization was performed through sequential four base pair shifts. Designed ASOs were used to treat cells for 48 h; after treatment, RNA was isolated. PCR was performed using the cDNA, and PCR products were separated on agarose gel. Gel band intensities were calculated, and the percentage of skipped product was analyzed. A combination of ASOs was also used for the optimization of treatments.

Cell Titer-Glo assay

Cells were seeded in 96-well plates and incubated for 24 h. They were treated with EGFR-targeted ASOs and the control ASO for 24, 48, 72, and 96 h. Cell viability was measured using the Cell Titer-Glo luminescent cell viability assay (Cat# G7570; Promega) as per the manufacturer's protocol.

Cell survival assay

A certain number of cells were seeded in 12-well plates for 24 h. They were treated with the control and targeted ASOs. After the wells had sufficient colonies, we removed the media and washed the wells with PBS. Cells were fixed with cold methanol for 10 min at −20°C. Methanol was removed, and 0.1% crystal violet was added to each well. The plate was shaken in a rocker for 30 min, and the wells were washed with water until the wash liquid became clear. Pictures of the wells were taken and analyzed. Crystal violet was extracted with methanol, and the absorbance was measured at 540 nm. The readings were used to calculate cell viabilities.

Western blotting

Cell pellets were extracted after treatment and used for protein isolation. A Macherey Nagel nucleospin RNA/Protein isolation kit (Cat# 740933) was used to isolate proteins. Manufacturer's recommendations were followed, and isolated proteins were frozen. Proteins were loaded (30 μg) and run on SDS-PAGE (sodium dodecyl sulfate–polyacrylamide gel electrophoresis). They were transferred to polyvinylidene difluoride membrane, blocked using 5% milk, and incubated with primary antibodies overnight at 4°C. After washing the unbound and excess primary antibodies, secondary antibodies were added for 1 h at room temperature. Following the incubation and washings, proteins were detected using SuperSignal West Pico plus chemiluminescent substrate (Cat# 34580; Thermo Fisher) and the Odyssey Fc instrument. β-Actin was used as the loading control.

Scratch assay

Cells (H292, PC9, and PC9GR) were seeded in a 96-well ImageLock plate separately at a density that resulted in 100% confluency the following day. The next day, the wound maker was used to create wounds in all the wells. After wounding, the media were aspirated immediately and washed twice with 1 × PBS. After washing, EGFR ASOs and controls were added with culture media to the respective wells. Finally, plates were placed in the IncuCyte live-cell analysis system and allowed to warm to 37°C for 30 min before scanning. The plates were scanned every 3 h for 3 to 5 days, and data were analyzed.

Sample preparation for proteomics/phosphoproteomics

Cells were lysed in denaturing lysis buffer containing 8 M urea, 20 mM HEPES (pH 8), 1 mM sodium orthovanadate, 2.5 mM sodium pyrophosphate, and 1 mM β-glycerophosphate. Protein pellets were resuspended for Bradford assay to estimate total protein content [Pierce™ Coomassie (Bradford) Protein Assay Kit, 23200; Thermo Scientific]. The proteins were reduced with 1/10 volume of 45 mM DTT for 20 min at 60°C and alkylated with 1/10 volume of 110 mM iodoacetamide for 15 min in the dark. Trypsin digestion was carried out at 37°C overnight, followed by additional trypsin the next morning for a 2-h incubation. Tryptic peptides were then acidified with 20% trifluoroacetic acid (TFA) for a final concentration of 1% TFA and desalted with C18 Sep-Pak cartridges as per the manufacturer's instructions (HyperSep C18 Cartridges, 60108-390; Thermo Scientific).

Tandem mass tag labeling

Lyophilized peptides (400 μg) from each sample were labeled with TMT10plex reagent (TMT10plex™ Isobaric Label Reagent Set, 90110; Thermo Scientific). The label incorporation was checked using liquid chromatography-tandem mass spectrometry (LC-MS/MS) and spectral counting; 98% or greater label incorporation was achieved for each channel. The reaction of the 10 samples was then quenched, pooled, and lyophilized.

High pH reversed-phase peptide separation

Following lyophilization, the peptides were redissolved in 250 μL of aqueous 20 mM ammonium formate, pH 10.0 (bRPLC A solvent). The high pH reversed-phase separation was performed on an XBridge 4.6 mm ID × 100 mm in length column packed with BEH C18 resin, 3.5 μm particle size, and 130 Å pore size (Waters) at a flow rate of 0.6 mL/min. The peptides were eluted as follows: 5% bRPLC solvent B for 10 min; 5% to 15% solvent B over 5 min; 15% to 40% solvent B over 47 min; 40% to 100% solvent B over 5 min; and held at 100% solvent B for 10 min, followed by re-equilibration at 1% solvent B.

Solvent A was composed of 5 mM ammonium formate in 2% acetonitrile at pH 10. Solvent B was 5 mM ammonium formate in 90% acetonitrile at pH 10. Three percent of the total separated peptides were concatenated into 24 fractions for protein expression and were dried in a vacuum centrifuge. The remaining 97% of peptides were concatenated into 12 fractions for phosphopeptide enrichment and were lyophilized.

Immobilized metal affinity chromatography enrichment

Fractionated peptides were redissolved in immobilized metal affinity chromatography (IMAC) loading buffer containing 85% acetonitrile with 0.1% TFA. The phosphopeptides in each fraction were enriched using IMAC resin (Cell Signaling Technology) on a KingFisher robot (Thermo Fisher). Briefly, the IMAC resin was washed once with loading buffer and the peptides were incubated with 130 μL of IMAC resin for 30 min at room temperature, with gentle agitation. After incubation, the IMAC resin was washed twice with loading buffer, followed by a single wash with wash buffer containing aqueous 80% acetonitrile with 0.1% TFA. The phosphopeptides were eluted with elution buffer containing, 2.5% ammonia in aqueous 50% acetonitrile. The phosphopeptides were dried using vacuum centrifugation and then resuspended in 20 μL of LC loading solvent [2% acetonitrile with 0.1% formic acid (FA)] for LC-MS/MS.

Liquid chromatography with tandem mass spectrometry

A nanoflow ultra-high performance liquid chromatograph and an electrospray benchtop orbitrap mass spectrometer (RSLC Q Exactive HF-X; Thermo, San Jose, CA) were used for tandem mass spectrometry peptide sequencing experiments. Peptides were first loaded onto a precolumn (100 μm ID × 2 cm in length packed with C18 reversed-phase resin, 5 μm particle size, and 100 Å pore size) and washed for 8 min with aqueous 2% acetonitrile containing 0.1% FA (solvent A).

The trapped peptides were eluted onto a C18, 75 μm ID × 25 cm, 2 μm, 100 Å analytical column (Dionex, Sunnyvale, CA) using a 120-min program at a flow rate of 300 nL/min of 5% solvent B (above) for 8 min; 5% to 38.5% solvent B over 90 min; and 50% to 90% solvent B over 7 min and held at 90% for 5 min, followed by 90% to 5% solvent B in 1 min, and re-equilibrated for 10 min. Solvent A was composed of 98% ddH_2O and 2% acetonitrile containing 0.1% FA. Solvent B was 90% acetonitrile and 10% ddH_2O containing 0.1% FA. Twenty tandem mass spectra were collected in a data-dependent manner following each survey scan. The

resolution settings were 60,000 and 45,000 for MS1 and MS/MS, respectively. The isolation window was 0.8 Th, with a 0.2 offset.

Data analysis

MaxQuant (version 1.5.2.8) was used to quantify the tandem mass tag reporter ion intensities. Spectra were assigned and quantitated using MaxQuant [20]. Data were further normalized using IRON [21] (iron_generic—proteomics) against the median sample (findmedian—spreadsheet—pearson). Biological replicates were averaged, and $\log_2$ ratios were calculated between treatment and control averages. *t*-Tests were then calculated from the individual biological replicates. Rows were determined to be differentially expressed if the following criteria were met: row maps to a human protein, $\log_2$ ratio $\geq \sim 0.585$ (1.5-fold) and P value <0.05.

Scores for each two-group comparison were calculated as the geometric mean of the $|\log_2 \text{ratio}|$ and $-\log10(P \text{ value})$

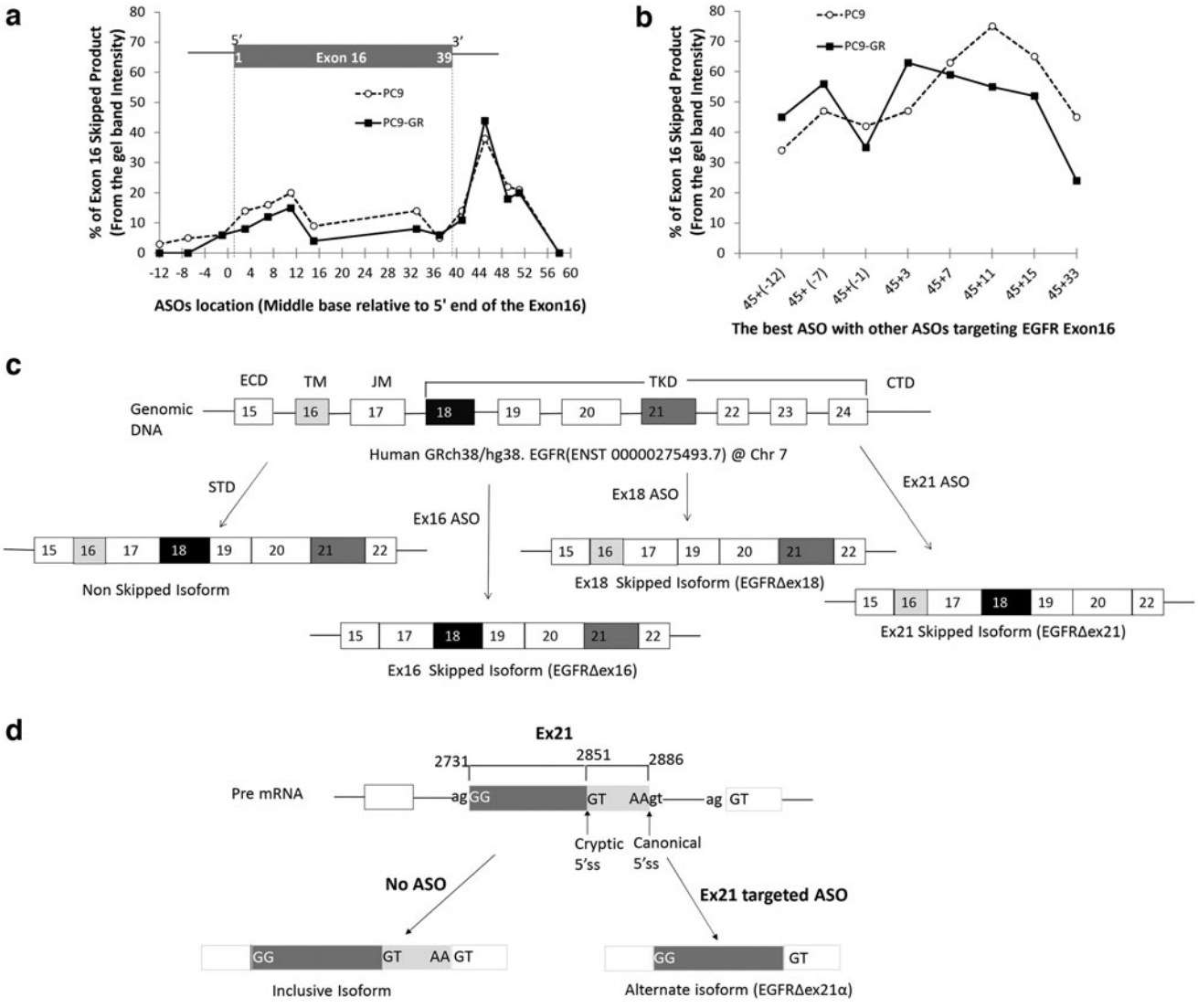

FIG. 1. Optimization of ASO target sequence and schematic diagram of human EGFR with its expected splice variants. To optimize exon 16 skipping, we systematically designed and tested *in vitro* ASOs centered on every fourth base pair near the 5′ and 3′ ends of exon 16. The x-axis shows the base pair location of the center of each ASO target relative to the start of exon 16. PC9 (*dashed line*) and PC9-GR (*solid line*) cells were exposed to 5 μM of EGFR ASOs for 48 h and quantified with respect to percent EGFR exon 16 skipped product (skipped/total) relative to the wild-type isoform by RT-PCR. We first examined **(a)** single ASOs, which revealed a distinct peak in efficacy for both cell lines centered on exon base pair 45 located with the 5′ splice site of intron 16 and a secondary peak within the 5′ exon centered on base pair 11. We then examined whether the ASO centered on base pair 45 could be combined with a second ASO to provide a synergistic effect **(b)**. Synergy was detected using a second ASO when it targeted the 5′ end of the exon (nonoverlapping) and a decreased efficacy when the second ASO was located near the original ASO (base pair 33) thought to be capable of sterically competing with the first ASO. **(c)** ASO targeting of exons 16 and 18 resulted in mRNA expression of the expected isoforms. In contrast, ASO targeting of exon 21 resulted in the use of a cryptic 5′ splice site formed within exon 21 that results in persistent inclusion of the 5′ portion of exon 21 **(d)**. ASO, antisense oligonucleotide; EGFR, epidermal growth factor receptor; RT-PCR, reverse transcriptase–polymerase chain reaction.

and were assigned the sign of the $\log_2$ ratio. Scores were then summed to generate a SumScore, with which to rank the upregulated and downregulated proteins. Pathway enrichment of differentially expressed proteins was performed against the Molecular Signatures Database (MSigDB) [22,23] gene lists using a Fisher's exact test after first filtering to remove any row mapping to proteins from multiple genes.

Results

Optimization of in vitro *ASOs in PC9 and PC9GR cell lines demonstrates ASO target sequence spatial relationship with splicing efficacy*

To investigate the impact of ASO target sequence on splice-switching efficacy, we used the ''*in vitro*'' formulation of ASOs, which refers to a specific chemical formulation of commercially available ASOs. These *in vitro* ASOs require the concomitant use of transfection agents and result in less effective splice switching, thereby providing a wide dynamic range in which we could investigate the impact of target sequence on ASO efficacy. *In vitro* ASOs placed within the 5′ splice site (to the right of exon 16) resulted in maximum exon exclusion (Fig. 1a, location 45).

In addition, *in vitro* ASOs targeting the region spanning the 3′ upstream intron and 5′ edge of the exon also resulted in modest splice switching (Fig. 1a). To assess for a potential synergistic effect of ASOs, we assessed the splicing efficacy of the most effective ASO in combination with other ASOs. Overall splicing efficacy was increased when the 5′ splice site ASO was combined with other effective 3′ ASOs, resulting in up to 80% splice switching in the PC9/PC9GR cell lines (Fig. 1b). Splicing efficacy either did not improve or decreased when ASO targets overlapped any portion of the same sequence, suggesting evidence for steric inhibition when applying ASOs with overlapping or competing target sequences.

Dose-dependent exon skipping was observed in H292, PC9, and PC9-GR cells

For subsequent investigations, we switched to the commercially available morpholino ''*in vivo*'' ASOs and found that the *in vivo* morpholino formulations provided dramatically increased, dose-dependent efficacy at comparable doses without the need for transfection agents. ASO administration resulted in dose-dependent exon skipping of exons 16 (EGFRΔex16/Fig. 1c) and 18 (EGFRΔex18/Fig. 1c), which resulted in complete exon skipping by 5 μM concentration in H292 cells (EGFR WT-OE, Fig. 2a, b). Similar results were observed with exon 18 in both PC9 (Fig. 2c) and PC9GR cells (Fig. 2d). Complete skipping of exon 16 in PC9 and PC9-GR cells was also observed at 5 μM (Supplementary Fig. S1).

In contrast, when we used human umbilical vascular endothelium cells (HUVEC) as control cell lines, we did not observe any skipping at mRNA levels (Supplementary Fig. S2a). The *in vivo* ASO formulations were used for all other experiments. Interestingly, ASOs targeting EGFR Ex21 did not form fully skipped isoform due to the use of a cryptic 5′ splice site (EGFRΔex21α; Supplementary Fig. S3 and Fig. 1d). Sequences of the novel mRNA isoforms were verified by Sanger DNA sequencing (GENEWIZ, South Plainfield, NJ).

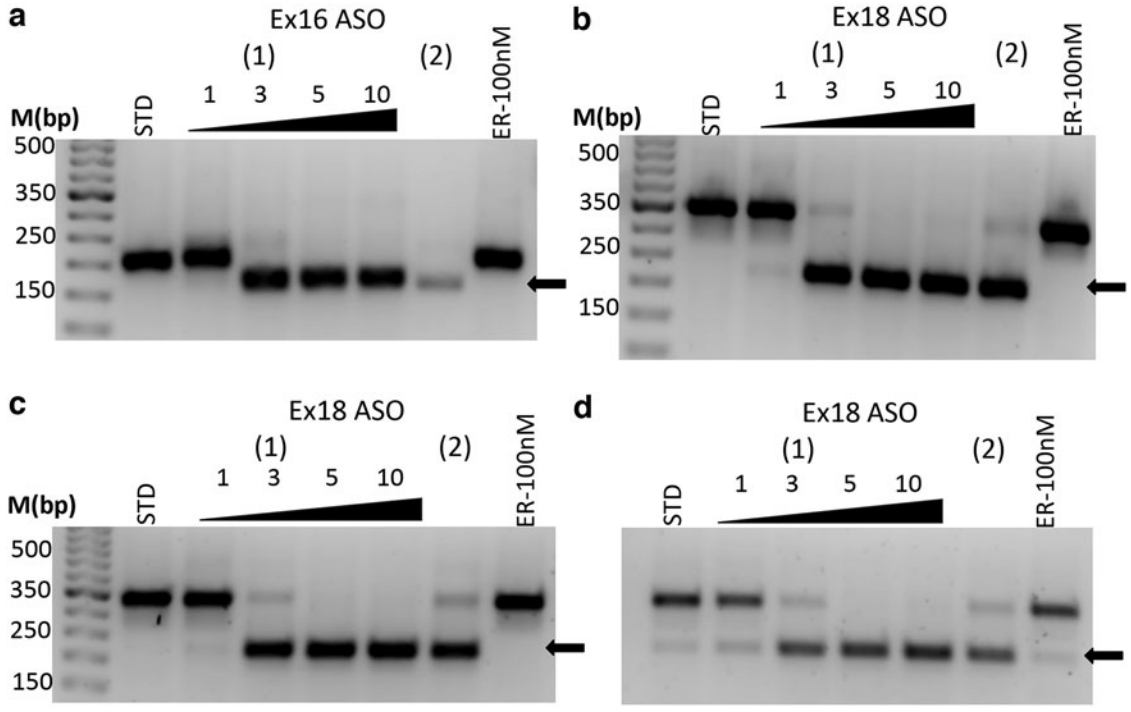

FIG. 2. *In vivo* ASOs induce dose-dependent complete skipping of targeted exons in multiple NSCLC cell lines. The *in vivo* ASO formulation showed significantly improved efficacy compared to the *in vitro* formulation (Fig. 1) and was able to induce complete targeted exon skipping in H292 cells of exon 16 **(a)** and exon 18 **(b)** and exon 18 in both PC9 **(c)** and PC9-GR **(d)**. ASOs were used as 0, 1, 3, 5, and 10 μM concentrations for 48 h. (1) Represents the optimized ASO and (2) is a secondary ASO at 5 μM. *Arrow* (*lower* bands) represents the skipped product. No effect was observed with erlotinib (ER). NSCLC, nonsmall cell lung cancer.

Cell growth was reduced in response to EGFR ASOs

Cell growth was reduced in response to ASOs as confirmed by cell viability, scratch, and colony-forming assays. Cell viability was significantly reduced with the induction of EGFRΔex16, EGFRΔex18, and the EGFRΔex21α isoforms. Cell viability decreased over time, with a maximum effect noted at 96 h for all three cell lines used (Fig. 3a–c). Interestingly, no significant effect on cell viability was observed in HUVEC control cell lines treated with EGFR ASOs (Supplementary Fig. S2b).

A cell survival assay further confirmed the cell viability reduction in response to EGFR ASOs targeting exons 16, 18,

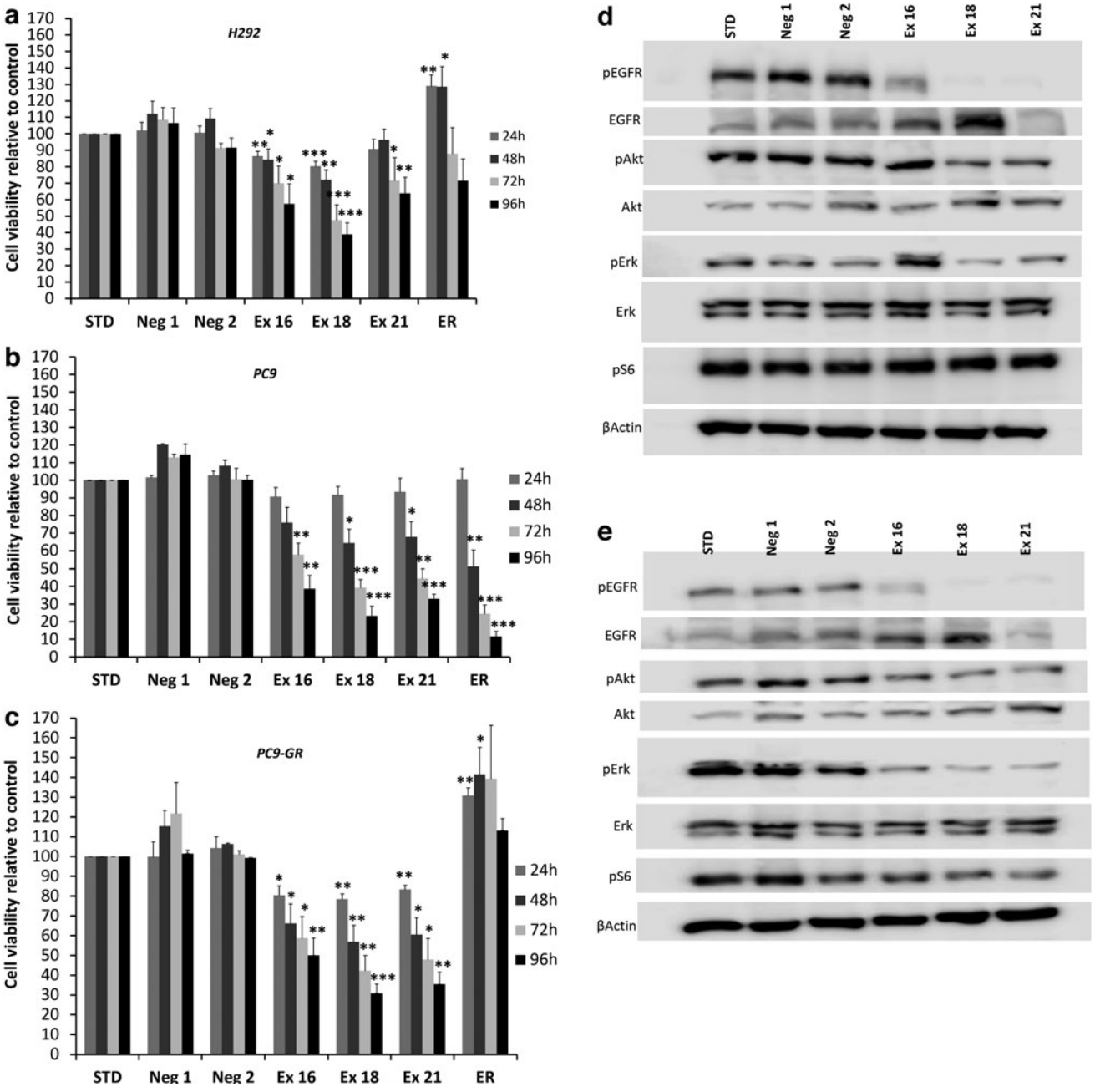

FIG. 3. ASO-induced skipping of exons 16, 18, and 21 results in reduced *in vitro* cell viability and EGFR signaling inhibition in H292, PC9, and PC9-GR cells. Cell viability was assessed in **(a)** H292, **(b)** PC9, and **(c)** PC9-GR cell lines measured using Cell Titer Glo Assay (Promega) and revealed that ASO targeting of exon 18 resulted in the largest reduction in cell viability across all three cell lines, whereas erlotinib only reduced viability in PC9 cells. Western blot analysis of **(d)** PC9 cells and **(e)** PC9-GR cells revealed that ASOs directed to the tyrosine kinase domain (exons 18 and 21) resulted in more profound suppression of EGFR signaling than targeting the transmembrane domain (exon 16). Blots show results for phosphorylation of EGFR on tyrosine (Y) 1,068, Akt at serine (S) 473, Erk targets at threonine (T) 202/tyrosine (Y) 204, and S6 at serine (S) 235/236. Cells were treated with 5 μM concentrations of the indicated ASOs and 100 nM erlotinib (ER). Neg1 and Neg2 are custom negative controls, and STD refers to the company-provided standard negative control. All the treatments lasted 48 h. *Asterisks* indicate two-tailed *t*-test significance using thresholds of $*P<0.05$, $**P<0.01$, and $***P<0.001$.

and 21 (Supplementary Fig. S4). Decreased growth and migration were observed in response to ASOs as assessed by scratch assay, especially in PC9 and PC9 GR cells (Supplementary Fig. S5). Interestingly, induction of EGFRΔex18, and EGFRΔex21α isoforms resulted in the robust reduction in cell migration.

EGFR pathway signaling was reduced in response to EGFR ASOs

EGFR and its downstream targets were downregulated in response to EGFR ASOs (Fig. 3d, e). Phosphorylated EGFR (pEGFR), phosphorylated Akt (pAkt), and phosphoErk (pErk) levels were significantly reduced when ASO targeted exons 18 and 21 in PC9 cells, and to a far lesser extent for exon 16 (Fig. 3d). pAkt and pErk were significantly reduced in response to the induction of EGFRΔex16, EGFRΔex18, and EGFRΔex21α isoforms in PC9-GR cells. The induction of EGFRΔex18 isoform and cryptic splice site isoform resulting from partial skipping of exon 21 (EGFRΔex21α) both significantly decreased pEGFR levels in PC9-GR cells (Fig. 3e).

Expression proteomics and phosphoproteomics show that EGFR ASOs activate pathways related to cell proliferation

Pathway enrichment of differentially expressed proteins significantly (P value $<10e^{-10}$) indicated ASO- and erlotinib-induced changes in cell cycle, mitosis, and G2/M checkpoint inhibition pathways. Proteomic analysis revealed that 13 out of 14 upregulated pathways and 4 out of 8 downregulated pathways overlapped in ASO-treated and erlotinib-treated PC9 cells, including cell growth-related pathways such as DNA replication, transcription, and the cell cycle (Fig. 4). Interestingly, phosphoproteomic pathway enrichment showed that several pathways related to cell growth were significantly downregulated in both ASO-treated and erlotinib-treated PC9 cells (Fig. 5), whereas most of these downregulated pathways were upregulated according to protein expression (Fig. 4).

In addition to these pathways, proteins involved in apoptosis and apoptotic cleavage pathways were hyperphosphorylated, further confirming the involvement of cell growth (Fig. 5). The EGFR downstream signaling pathway was significantly hypophosphorylated in cells treated with EGFR ASOs (Supplementary Fig. S6), confirming EGFR-specific inhibition by EGFR-targeted ASO treatment. Most phosphorylation sites on EGFR were hypophosphorylated following both ASO and erlotinib treatment; however, S1026 and S1081 were unique serine sites that were significantly hypophosphorylated in EGFR ASO-treated cells, while hyperphosphorylated in erlotinib-treated cells (Supplementary Fig. S6).

Discussion

In this study, we describe a novel, splicing-based approach to inhibit EGFR (SAKI) and demonstrate its ability to inhibit

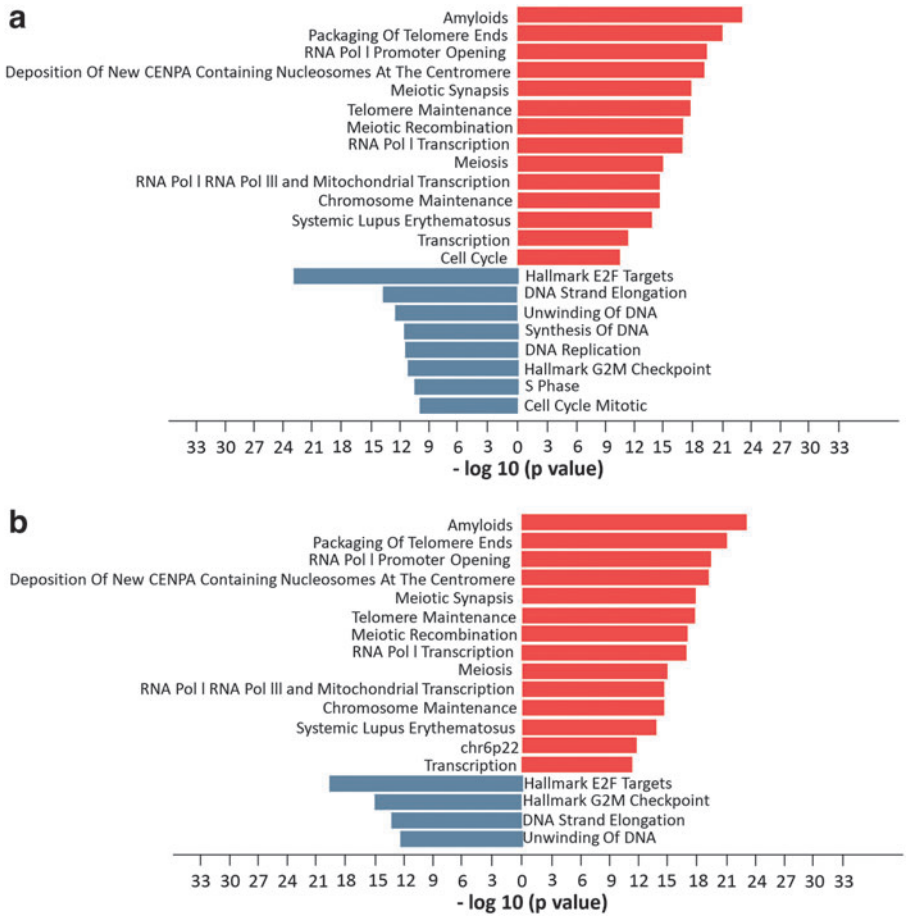

FIG. 4. Pathway enrichment analysis of **(a)** combined proteomic analysis following EGFR ASO 16, 18, and 21 treatment compared with standard ASO control (STD) in PC9 cells. Comparable pathway enrichment was observed following **(b)** direct inhibition of EGFR using erlotinib treated relative to STD. Analysis was performed using the DE proteins. Figures represent pathways that enriched for increased (*red*) and decreased (*blue*) protein expression. All pathways have negative log10 P values >10. DE, differentially expressed.

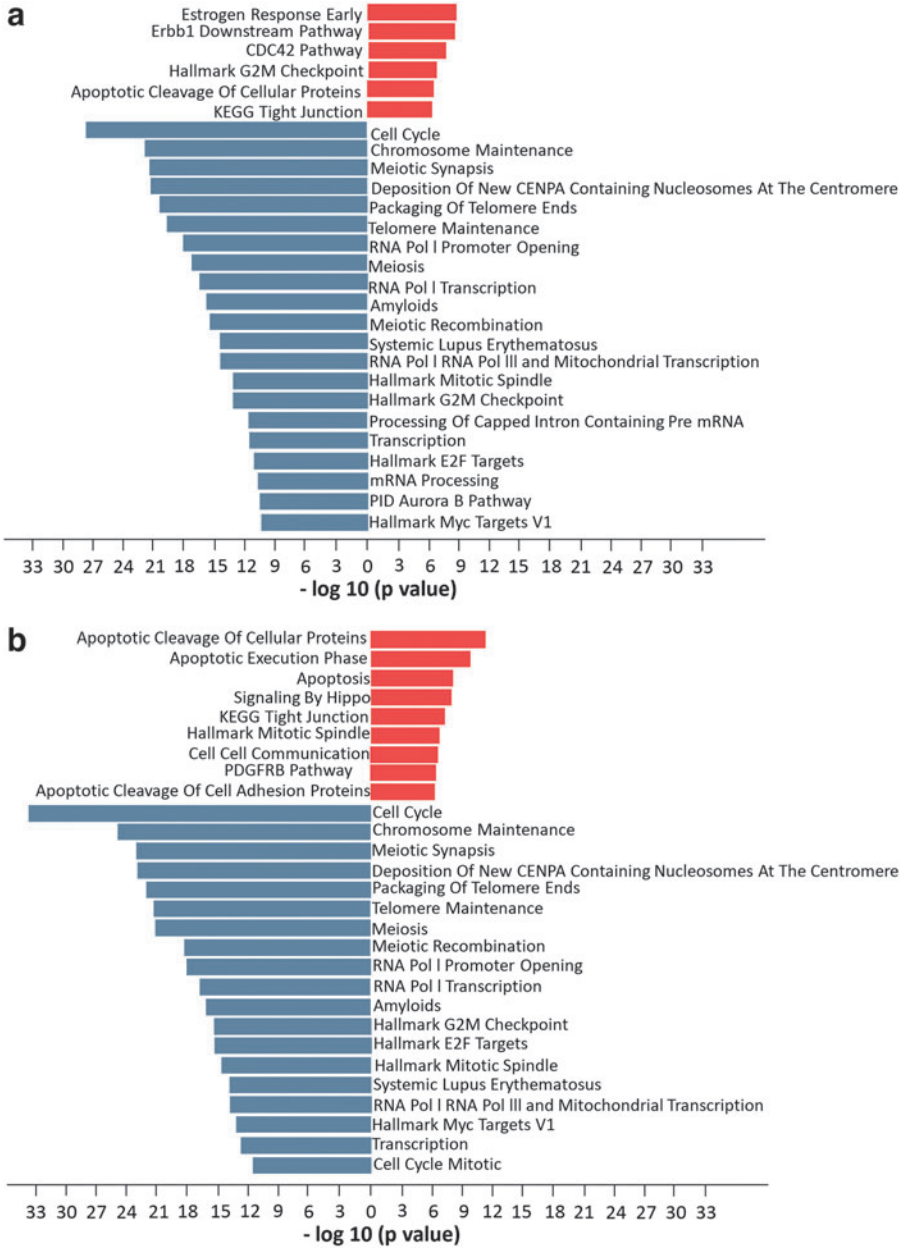

FIG. 5. Pathway enrichment analysis of **(a)** combined phosphoproteomic analysis following EGFR ASO 16, 18, and 21 treatment compared with standard ASO control (STD) in PC9 cells reveals inhibition of cell cycle and transcription and upregulation of apoptosis and EGFR (Erbb1) downstream pathways. Comparable pathway enrichment was observed following **(b)** direct inhibition of EGFR using erlotinib treated relative to STD. Analysis was performed using the DE proteins. Figures represent pathways that are formed only using upregulated DE proteins (*red*) and downregulated DE proteins (*blue*). All pathways were selected based on negative log10 *P* values >10.

in vitro oncogenic phenotypes and EGFR signaling in both TKI-resistant EGFRmt and EGFR WT-OE NSCLC cell models.

We successfully optimized custom ASO sequences to drive the exclusion of exons 16 (transmembrane domain), 18, and the 5′ half of 21 (tyrosine kinase domain) to generate new mRNA EGFR isoforms with predicted dominant negative activity (Fig. 1c). We were unable to directly detect expression of the skipped protein isoforms due to technical limitations because of the small size of excluded exons relative to the full-length protein. We also conducted mass spectrometry to investigate the expression of EGFR novel isoforms at the protein level, but were not able to identify peptide fragment mapping to the novel isoforms in *post hoc* proteomic analysis. This could be due to technical limitations of mass spectrometry when focusing on a small target region or could indicate a lack of protein-level expression of the proposed EGFR isoforms.

However, if the dominant negative EGFR isoforms are not expressed at the protein level, it is not immediately clear how ASOs would be able to otherwise drive EGFR-specific changes in signaling, while maintaining stable EGFR total protein expression, which would suggest that simple knockdown or nonsense-mediated degradation of EGFR protein is not the mechanism of ASO-mediated EGFR inhibition. Finally, we did not observe toxicity in HUVEC, suggesting specificity by tissue type, which would be necessary to confer a therapeutic benefit.

There are several preclinical studies to develop ASOs that target oncogenes, such as HER2 and Bcl-x, but there are no reported studies on the EGFR gene [14,15]. Our data indicate that EGFR signaling can be inhibited in NSCLC mtEGFR as well as WT-OE EGFR using EGFR-targeted morpholino-based ASOs. The application of ASOs in the treatment of genetic diseases dates back three decades. Although we focused on the use of ASOs to exclude targeted exons, ASOs

are also capable of altering mRNA isoforms by selection of alternative 5′ transcription start sites, exon inclusion, and intron retention.

The first FDA-approved ASO drug was fomivirsen, a phosphorothioate-modified oligonucleotide, which was approved in 1998 for cytomegalovirus retinitis [24]. Mipomersen was the first FDA-approved systemically delivered ASO (in 2013) [25], and it was used to treat familial hypercholesterolemia by reducing the ApoB gene [26]. In 2016, two ASO drugs were approved by the FDA: eteplirsen, for Duchenne muscular dystrophy, and nusinersen, for spinal muscular atrophy [19,27,28].

Nusinersen is a 2′-*O*-methoxyethyl phosphorothioate derivative ASO that acts by including exon 7 in the SMN2 gene, which enhances the SMA full-length protein [28,29]. Eteplirsen is the only FDA-approved morpholino-based oligomer, and it is able to induce skipping of exon 51 of the dystrophin gene. Morpholino-derived ASOs have added advantages, such as higher stability and easy delivery. The ASOs were produced by morpholino-based chemistry (Genetool), and they are designed to skip certain exons of EGFR during the splicing process. These morpholino oligos consist of methylenemorpholine rings and nonionic phosphorodiamidate linkages. This uncharged backbone makes them stable to nucleases [30,31]. Vivo-morpholinos used in our research are uniquely designed with octa-guanidine dendrimers for improved delivery without transfection reagents [30].

Further studies are warranted to explore the synergistic effect of ASOs and TKIs, for example, whether the addition of ASOs to TKIs is capable of preventing or delaying development of known pathways of TKI resistance. Although we focused our ASO-based approach on EGFR, other oncogenes could also be investigated, particularly those which are currently considered undruggable targets. Finally, *in vivo* studies and pharmacokinetic modeling will be required to further assess the potential for EGFR-targeted ASOs before its consideration in clinical trials.

Acknowledgments

We greatly appreciate the Analytical Microscopy Core and the Proteomics & Metabolomics Core staff at Moffitt Cancer Center and Research Institute for their assistance. Moffitt core facilities are funded, in part, by the NCI through a Cancer Center Support Grant (P30-CA076292). We are also thankful to the Moffitt Scientific Editing Department for assistance in editing the article.

Author Disclosure Statement

T.R. holds a patent related to the therapeutic use of antisense oligonucleotides.

Financial Information

Timothy Robinson: DOD LCRP Career development grant.

Eric Welsh and Lancia N.F. Darville: Account: 5P30 CA076292-22 (PI: J. Cleveland Source: NIH/NCI Dates: February 18, 1998, to January 31, 2022 Title: H. Lee Moffitt Cancer Center and Research Institute Support Grant).

Charles E. Chalfant: National Institutes of Health grants R01 DK126444 (to Charles E. Chalfant). This work was also supported by research grants from the Veteran's Administration [VA Merit Review I, BX001792 (Charles E. Chalfant) and a Senior Research Career Scientist Award, IK6BX004603 (Charles E. Chalfant)]. The contents of this article do not represent the views of the Department of Veterans Affairs or the United States Government.

Supplementary Material

Supplementary Figure S1
Supplementary Figure S2
Supplementary Figure S3
Supplementary Figure S4
Supplementary Figure S5
Supplementary Figure S6

References

1. Manning G, DB Whyte, R Martinez, T Hunter and S Sudarsanam. (2002). The protein kinase complement of the human genome. Science 298:1912–1934.
2. Blume-Jensen P and T Hunter. (2001). Oncogenic kinase signalling. Nature 411:355–365.
3. Hubbard SR. (1999). Structural analysis of receptor tyrosine kinases. Prog Biophys Mol Bio 71:343–358.
4. Yarden Y and G Pines. (2012). The ERBB network: at last, cancer therapy meets systems biology. Nat Rev Cancer 12: 553–563.
5. Li SQ, KR Schmitz, PD Jeffrey, JJW Wiltzius, P Kussie and KM Ferguson. (2005). Structural basis for inhibition of the epidermal growth factor receptor by cetuximab. Cancer Cell 7:301–311.
6. Saadeh CE and HS Lee. (2007). Panitumumab: a fully human monoclonal antibody with activity in metastatic colorectal cancer. Ann Pharmacother 41:606–613.
7. Gonzalez-Larriba JL, M Lazaro-Quintela, M Cobo, M Domine, M Majem and R Garcia-Campelo. (2017). Clinical management of epidermal growth factor receptor mutation-positive non-small cell lung cancer patients after progression on previous epidermal growth factor receptor tyrosine kinase inhibitors: the necessity of repeated molecular analysis. Transl Lung Cancer Res 6 (Suppl 1): S21–S34.
8. Yoshida T, L Song, Y Bai, F Kinose, J Li, KC Ohaegbulam, T Munoz-Antonia, X Qu, S Eschrich, *et al.* (2016). ZEB1 mediates acquired resistance to the epidermal growth factor receptor-tyrosine kinase inhibitors in non-small cell lung cancer. PLoS One 11:e0147344.
9. Janne PA, J Son, I Voccia, M Uttenreuther-Fischer and K Park. (2015). Phase II study of BI1482694 in patients (pts) with T790M-positive non-small cell lung cancer (NSCLC) after treatment with an epidermal growth factor receptor tyrosine kinase inhibitor (EGFR TKI). Ann Oncol 26:145.
10. Niederst MJ, HC Hu, HE Mulvey, EL Lockerman, AR Garcia, Z Piotrowska, LV Sequist and JA Engelman. (2015). The allelic context of the C797S mutation acquired upon treatment with third-generation EGFR inhibitors impacts sensitivity to subsequent treatment strategies. Clin Cancer Res 21:3924–3933.
11. Hirsch FR, M Varella-Garcia, PA Bunn, MV Di Maria, R Veve, RM Bremnes, AE Baron, C Zeng and WA Franklin. (2003). Epidermal growth factor receptor in non-small-cell lung carcinomas: correlation between gene

copy number and protein expression and impact on prognosis. J Clin Oncol 21:3798–3807.
12. Oltean S and DO Bates. (2014). Hallmarks of alternative splicing in cancer. Oncogene 33:5311–5318.
13. Robinson TJ, MA Dinan, M Dewhirst, MA Garcia-Blanco and JL Pearson. (2010) SplicerAV: a tool for mining microarray expression data for changes in RNA processing. BMC Bioinformatics 11:108.
14. Wan J, P Sazani and R Kole. (2009). Modification of HER2 pre-mRNA alternative splicing and its effects on breast cancer cells. Int J Cancer 124:772–777.
15. Taylor JK, QQ Zhang, JR Wyatt and NM Dean. (1999). Induction of endogenous Bcl-xS through the control of Bcl-x pre-mRNA splicing by antisense oligonucleotides. Nat Biotechnol 17:1097–1100.
16. Ciardiello F, R Caputo, T Troiani, G Borriello, ER Kandimalla, S Agrawal, J Mendelsohn, AR Bianco and G Tortora. (2001). Antisense oligonucleotides targeting the epidermal growth factor receptor inhibit proliferation, induce apoptosis and cooperate with cytotoxic drugs in Human cancer cell lines. Int J Cancer 93:172–178.
17. Bauman J, N Jearawiriyapaisarn and R Kole. (2009). Therapeutic potential of splice-switching oligonucleotides. Oligonucleotides 19:1–13.
18. Gao QQ, E Wyatt, JA Goldstein, P LoPresti, LM Castillo, A Gazda, N Petrossian, JU Earley, M Hadhazy, *et al.* (2015). Reengineering a transmembrane protein to treat muscular dystrophy using exon skipping. J Clin Invest 125: 4186–4195.
19. Silver Spring, MD. FDA grants accelerated approval to first targeted treatment for rare Duchenne muscular dystrophy mutation [news release]. https://www.fda.gov/news-events/press-announcements/fda-grants-accelerated-approval-first-targeted-treatment-rare-duchenne-muscular-dystrophy-mutation Accessed December 13, 2019.
20. Tyanova S, T Temu and J Cox. (2016). The MaxQuant computational platform for mass spectrometry-based shotgun proteomics. Nat Protoc 11:2301–2319.
21. Welsh EA, SA Eschrich, AE Berglund and DA Fenstermacher. (2013). Iterative rank-order normalization of gene expression microarray data. BMC Bioinformatics 14:153.
22. Subramanian A, P Tamayo, VK Mootha, S Mukherjee, BL Ebert, MA Gillette, A Paulovich, SL Pomeroy, TR Golub, ES Lander and JP Mesirov. (2005). Geneset enrichment analysis: a knowledge-based approach for interpreting genome-wide expression profiles. Proc Natl Acad Sci U S A 102:15545–15550.
23. Liberzon A, C Birger, H Thorvaldsdottir, M Ghandi, JP Mesirov and P Tamayo. (2015). The molecular Signatures database hallmark gene set collection. Cell Syst 1:417–425.
24. Roehr B. (1998). Fomivirsen approved for CMV retinitis. J Int Assoc Physicians AIDS Care 4:14–16.
25. Product label approved by the U.S. Food and Drug Association for Kynamro, NDA no. 203568. www.accessdata.fda.gov/drugsatfda_docs/label/2013/203568s000lbl.pdf Accessed May 10, 2013.
26. Disterer P, R Al-Shawi, S Ellmerich, SN Waddington, JS Owen, JP Simons and B Khoo. (2013). Exon skipping of hepatic APOB pre-mRNA with splice-switching oligonucleotides reduces LDL cholesterol in vivo. Mol Ther 21: 602–609.
27. U.S. Food and Drug Administration. FDA approves first drug for spinal muscular atrophy. www.fda.gov/NewsEvents/Newsroom/PressAnnouncements/ucm534611.htm?source=govdelivery&utm_medium=email&utm_source=govdelivery Accessed January 3, 2017.
28. Ottesen EW. (2017). ISS-N1 makes the First FDA-approved drug for spinal muscular atrophy. Transl Neurosci 8:1–6.
29. Singh RN and NN Singh. (2018). Mechanism of splicing regulation of spinal muscular atrophy genes. Adv Neurobiol 20:31–61.
30. Morcos PA, Y Li and S Jiang. (2008). Vivo-Morpholinos: a non-peptide transporter delivers Morpholinos into a wide array of mouse tissues. Biotechniques 45:613–614.
31. Moulton JD. (2017). Making a morpholino experiment work: controls, favoring specificity, improving efficacy, storage, and dose. Methods Mol Biol 1565:17–29.

Address correspondence to:
Timothy J. Robinson, MD, PhD
Department of Therapeutic Radiology
Yale School of Medicine
15 York Street
Hunter Building 308
New Haven, CT 06510
USA

E-mail: timothy.j.robinson@yale.edu

Received for publication November 11, 2021; accepted after revision April 21, 2022; Published Online July 20, 2022.

Supplemental Figure S1. PCR validation following exposure to in vivo ASOs targeting Exon 16 and 18 targeted demonstrates complete exclusion of exons 16 (left two groups) and 18 (right two groups), respectively, in both PC9 and PC9-GR cells. ASO exposure using 5 μM concentrations for 48h. PCR products were run on 2.5% agarose Gel. Neg1 and Neg 2 are negative controls.

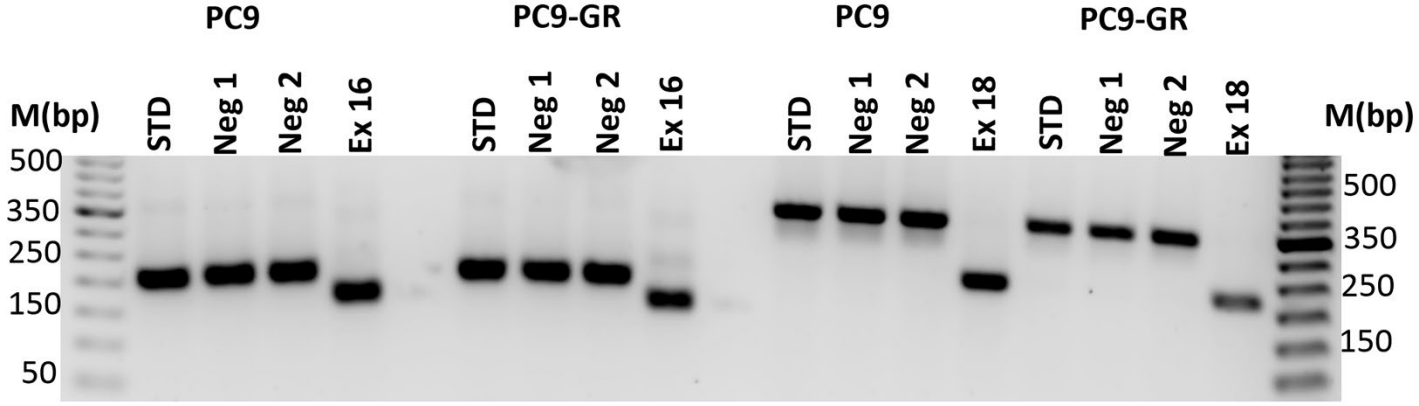

Supplemental Figure S2. HUVEC cells show no evidence of decreased viability following EGFR ASO treatment**. (a)** PCR results of EGFR ASOs targeting exons 16, 18, and 21 **(b)** HUVEC cell viability in response to EGFR ASOs treatment. ASOs used as 5 μM concentrations for 48 h. PCR products were run on 2.5% agarose Gel. ASOs used as 5 μM concentrations for 48 h. PCR products were run on 2.5% agarose Gel. Cell viability was measured using Cell Titer Glo Assay (Promega). Cells were treated with indicated ASOs at 5 μM concentrations for different time points. Neg1 and Neg2 are negative controls, STD refers to the standard control.

a)

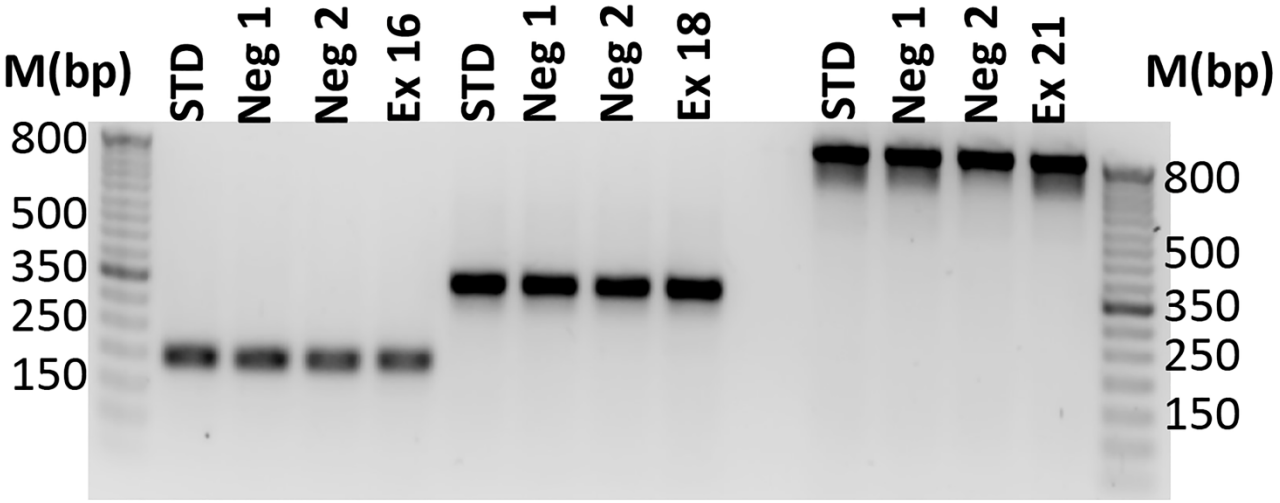
M(bp)
STD
Neg 1
Neg 2
Ex 16
STD
Neg 1
Neg 2
Ex 18
STD
Neg 1
Neg 2
Ex 21
M(bp)
800
500
350
250
150
800
500
350
250
150

b)

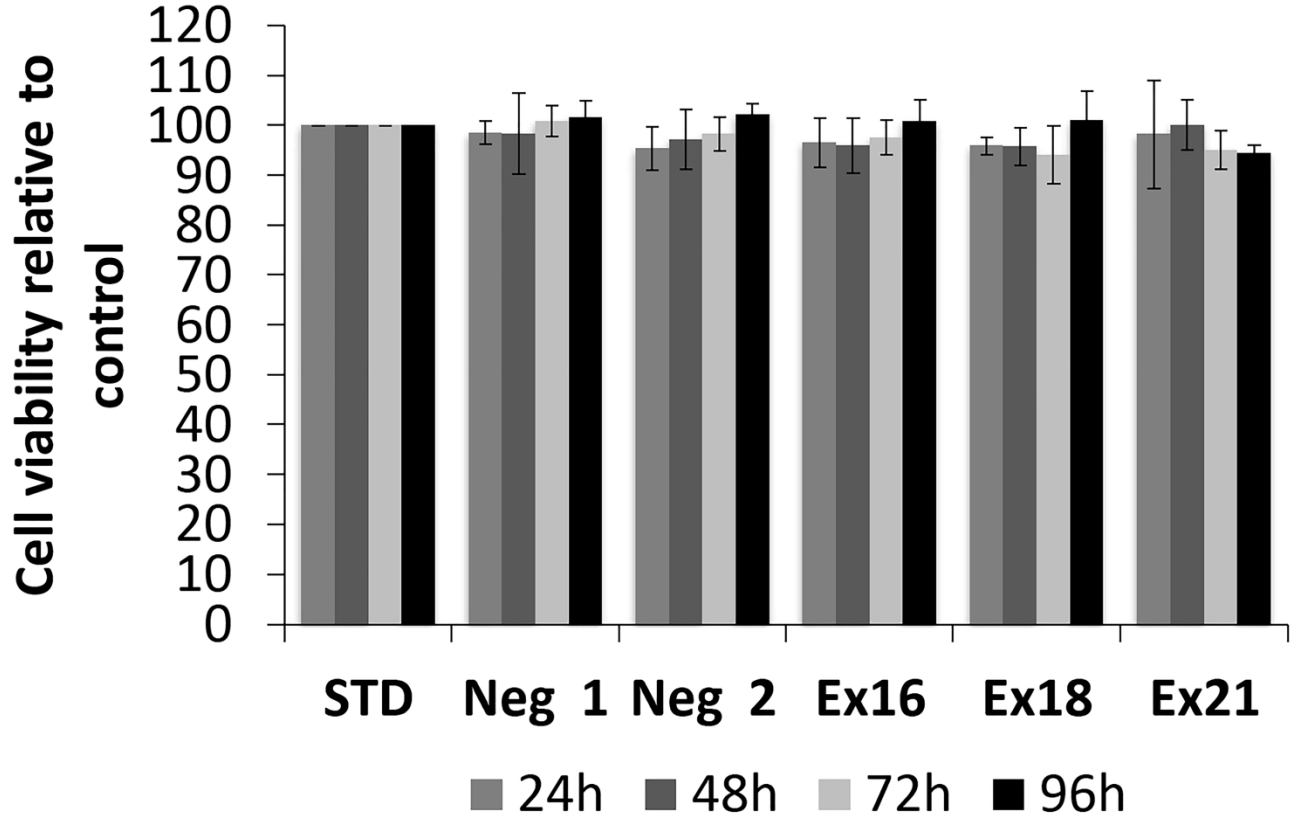
Cell viability relative to control
120
110
100
90
80
70
60
50
40
30
20
10
0
STD
Neg 1
Neg 2
Ex16
Ex18
Ex21
24h
48h
72h
96h

Supplemental Figure S3. PCR validation of exon skipping in samples sent for proteomic analysis. Exon 16, 18 and 21 targeted EGFR vivo ASOs introduced into PC9 cells. ASOs used as 5 μM concentrations for 72h except ER, used at 100 nM. PCR products were run on 2.5% agarose Gel. ER stands for erlotinib. Left and right figures represent two passages of PC9.

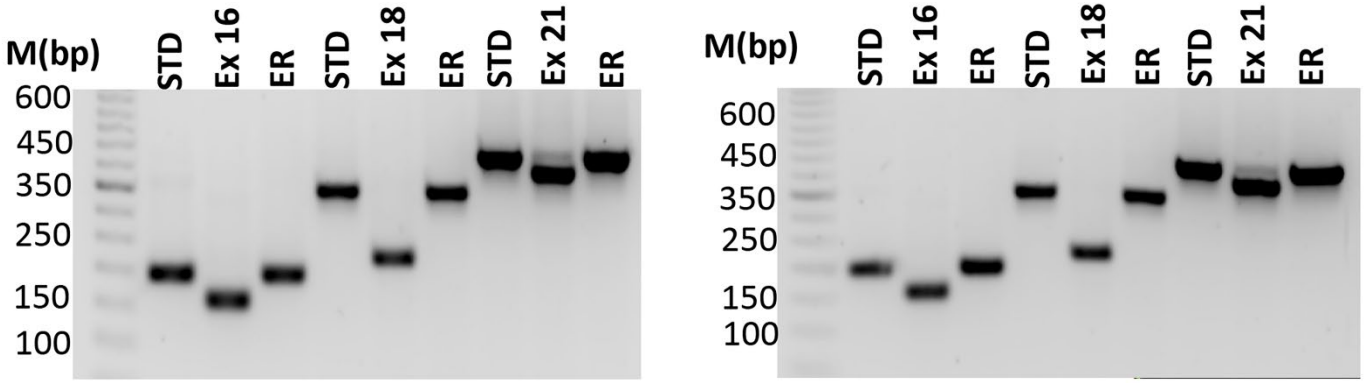

Supplemental Figure S4. Survival assays confirm ASO-based growth inhibition in **(a)** H292 cells, **(b)** PC9 cells and **(c)** PC9-GR cells. Cells were treated with STD, Negative controls, ER and Exon 16, 18 and 21 targeted vivo ASOs. All ASOs were used at 5 μM concentrations. ER: Erlotinib used at 100 nM concentration. NT: not treated.

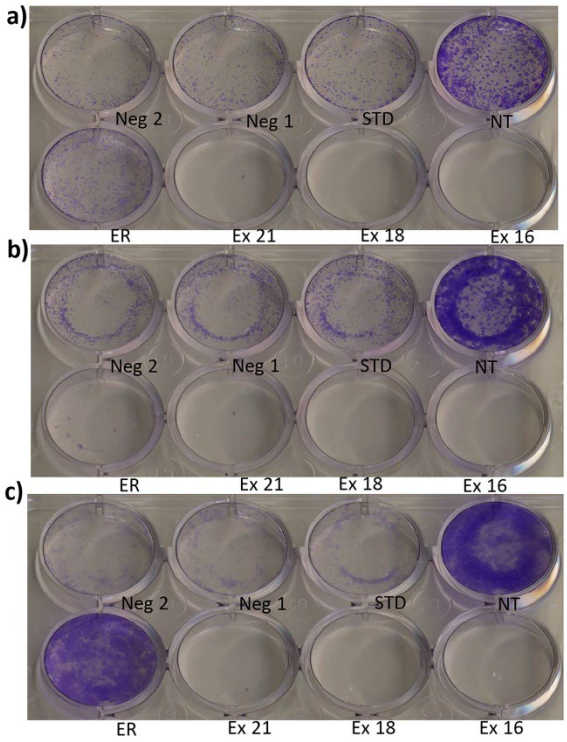

Supplemental Figure S5. Scratch assays show delayed wound healing following ASO treatment in **(a)** H292 cells, **(b)** PC9 cells and **(c)** PC9-GR cells, but showed the largest effect when exons 18 or 21 (vs. 16) were targeted. Cells were treated with indicated vivo ASOs for the entire duration of the experiment at 5 μM concentrations. The scan was performed in the IncuCyte every 3 hrs. Data represent three independent experiments.

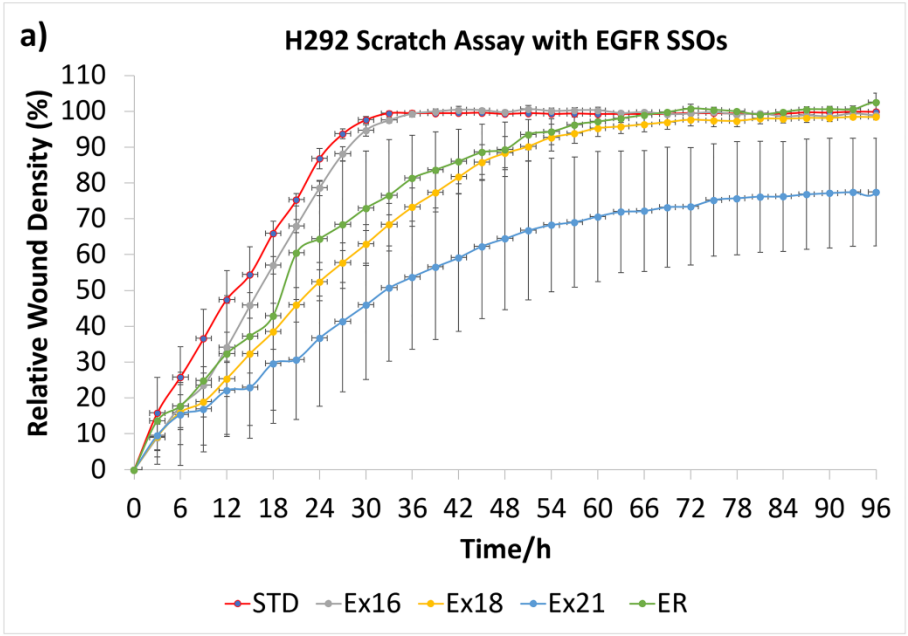
a)
H292 Scratch Assay with EGFR SSOs
Relative Wound Density (%)
0 10 20 30 40 50 60 70 80 90 100 110
0 6 12 18 24 30 36 42 48 54 60 66 72 78 84 90 96
Time/h
STD Ex16 Ex18 Ex21 ER

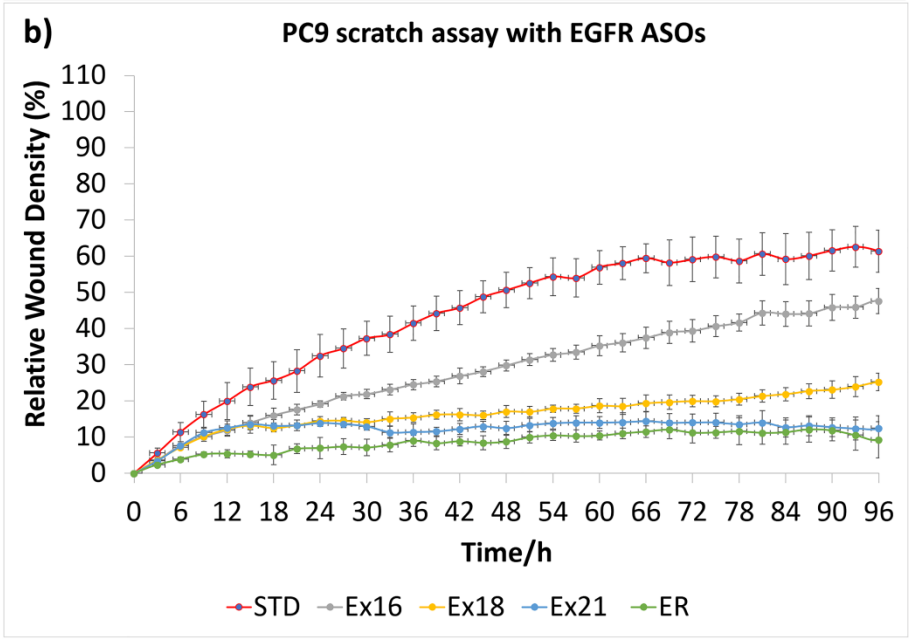
b)
PC9 scratch assay with EGFR ASOs
Relative Wound Density (%)
0 10 20 30 40 50 60 70 80 90 100 110
0 6 12 18 24 30 36 42 48 54 60 66 72 78 84 90 96
Time/h
STD Ex16 Ex18 Ex21 ER

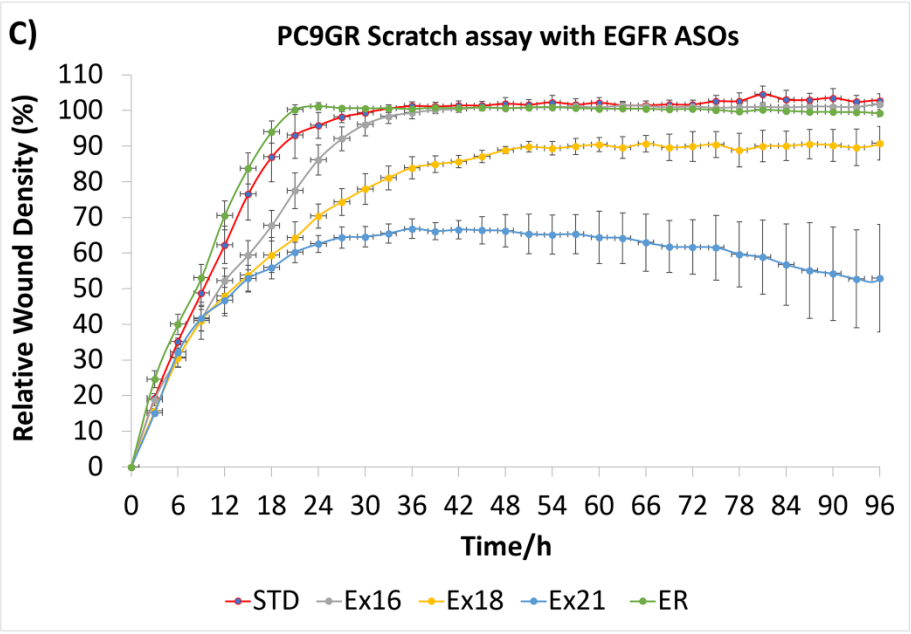
C)
PC9GR Scratch assay with EGFR ASOs
Relative Wound Density (%)
0 10 20 30 40 50 60 70 80 90 100 110
0 6 12 18 24 30 36 42 48 54 60 66 72 78 84 90 96
Time/h
STD Ex16 Ex18 Ex21 ER

Supplemental Figure S6. Phosphoproteomic analysis of EGFR phosphorylation changes in Serine (S) Threonine (T) and Tyrosine (Y) sites. **a)** A model showing the location of phosphorylated sites observed in the phosphoproteomic analysis **b)** Relative fold changes of the phosphorylation.